Supporting Information

Ichikawa et al. 10.1073/pnas.1119338109

SI Materials and Methods

Cell Culture. Neonatal rat cardiomyocytes (NRCMs) were prepared from 1- to 2-d-old Sprague–Dawley rats and cultured as described previously (1).

Generation of ABCB8 loxP and ABCB8$^{\Delta/\Delta}$ Mice. A mouse 129/Svj BAC genomic library was screened with a 1-Kb fragment corresponding to an area around ABCB8 exon 1. The BAC clones containing exon 1 were used to construct the targeting vector using the recombineering technique (2). To generate mice with cardiac-specific ABCB8 ablation (ABCB8$^{\Delta/+}$ or ABCB8$^{\Delta/\Delta}$), heterozygous MER-Cre-MER (MCM) transgenic mice (3) were bred with MCM × ABCB8$^{f/+}$ or MCM × ABCB8$^{f/f}$ mice, followed by oral administration of tamoxifen chow (30 mg/kg/d by mouth for 2 wk). Sex-matched littermate controls were used for each analysis. The animal studies were conducted in accordance with Northwestern University animal care guidelines.

Cardiac Function Analysis. Echocardiography was performed by using a Vevo 770 high-resolution imaging system. The parasternal short- and long-axis views were used to obtain 2D and M-mode images. Hemodynamic parameters were analyzed on a high-fidelity 1.2-F transducer-tipped pressure-volume catheter (Scisense). For end-systolic pressure and end-diastolic pressure, the catheter was inserted into the left ventricle and pressure recordings were obtained. Heart rate was measured under anesthesia.

Histochemical Analysis. Fiber morphology was assessed with H&E and heart fibrosis was assessed by Masson trichrome. The in situ cell death detection kit, Fluorescein (Roche Diagnostics), was used for TUNEL staining. Deparaffinized heart sections were stained using Prussian Blue Reaction for the Demonstration of Iron Kit (Polysciences).

Transmission EM. Cardiac tissue from left ventricle free wall was fixed in 2.5% glutaraldehyde and 2.0% paraformaldehyde in 0.1 M sodium cacodylate buffer at 4 °C, washed in cold 0.1 M cacodylate buffer, treated with 2% osmium tetroxide in 0.1 M sodium cacodylate, en-bloc stained in 3% aqueous uranyl acetate, dehydrated through a series of ascending grades of ethanol, and embedded in the epoxy–araldite resin. Thin sections of 70 nm were cut with a Leica UC6 ultramicrotome and examined with a FEI Tecnai Spirit transmission electron microscope. Mitochondrial size was analyzed with ImageJ software.

Cell Viability. NRCMs were treated with 50 μM H_2O_2 for 16 h, and cell viability was assessed by a CellTiter 96 Aqueous Nonradioactive Cell Proliferation Assay Kit (Promega).

Western Blot. Protein (15–20 μg) was resolved on SDS/PAGE gels and transferred to nitrocellulose membranes (Invitrogen). The membranes were probed with antibodies against ABCB8 (4), actin, GAPDH, GFP (Santa Cruz), complex II subunits 30 kDa and 70 kDa (Invitrogen), ABCB7, and tubulin (Abcam). HRP-conjugated donkey anti-rabbit and donkey anti-mouse were used as secondary antibodies (Santa Cruz) and visualized by Pierce SuperSignal chemiluminescent substrates.

RT-PCR. RNA was isolated by using RNA STAT-60 (Tel-Test), reverse-transcribed with a Random Hexamer (Applied Biosystems), and amplified on a 7500 Fast Real-Time PCR system with SYBR Green PCR Master Mix (Applied Biosystems). Primer sequences are reported in Table S1. The relative expression of each mRNA was calculated by the comparative threshold cycle method and normalized to 18S rRNA.

Isolation of Mitochondria. A Mitochondrial Isolation Kit for Tissue or Cultured Cells (Pierce) was used to purify mitochondrial fraction according to the manufacturer's protocol. Membrane potential of isolated mitochondria was assessed by staining with 5 μM rhodamine 123 (Sigma) for 15 min, followed by flow cytometry.

Measurement of Iron. The total mitochondrial nonheme iron was assessed spectrophotometrically as a formation of Fe(II)–bathophenanthroline disulfonate complex (5). For determination of mitochondrial ^{55}Fe content, cells were incubated with 100 to 250 nM ^{55}Fe (Perkin-Elmer) conjugated to nitrilotriacetic acid (^{55}Fe-NTA) for 48 h. Cells and mitochondria were washed with cold 500 μM bathophenanthroline sulfonate in PBS solution to remove membrane-associated ^{55}Fe. Radioactivity was quantified on a Beckman scintillation counter. Heme content was quantified as fluorescence of protoporphyrin IX at 405 nm/600 nm excitation/emission wavelengths as described previously (6). Iron levels were normalized to mitochondrial protein.

Enzyme Activity Assay. Xanthine oxidase activity was measured using the Amplex red H_2O_2 assay kit (Molecular Probes). Complex II activity was measured by using Complex II Enzyme Activity Microplate Assay Kit (MitoSciences). Complex I and IV activities were measured using the Sandwich ELISA Kit–Dipsticks assay (MitoSciences). For aconitase activity, mitochondria were incubated in a reaction buffer containing *cis*-aconitate, isocitrate dehydrogenase, and NADP at 30 °C for 45 min, and α-ketoglutarate content was measured at 340 nm. Enzymatic activities were normalized to cellular protein concentration.

siRNA and Adenoviral Treatment of Cells. The target or nonsilencing siRNA were transfected into NRCMs by using a TransMessenger Transfection Kit (Qiagen). For ABCB8 down-regulation in NRCMs, an siRNA validated previously was used (1). HEK293 were transfected with a pool of three siRNAs against ABCB8. Overexpression was achieved with adenoviral transduction of human ABCB8 or GFP (1). This adenovirus was derived from the AdCIG vector, and contains the human ABCB8 cDNA under CMV promoter with an internal ribosomal entry site between the ABCB8 and GFP cDNAs. Thus, the GFP protein does not localize with ABCB8. Each adenovirus at a multiplicity of infection of 5 was used in overexpression experiments unless noted otherwise.

Measurement of ROS. MitoSox red (Invitrogen) was used to assess mitochondrial $O_2^{\cdot}$ production (7) and analyzed by confocal microscopy or FACS in a FACSCanto flow cytometer (BD Bioscience). For lipid peroxidation assay, malondialdehyde and 4-hydroxyalkenals concentrations were determined by using a commercially available Lipid Peroxidation Microplate Assay Kit (Oxford Biomedical Research).

Iron 55 Export Assay. For iron export, HEK293 cells were incubated with 100 to 250 nM ^{55}Fe conjugated to nitrilotriacetic acid for 48 h. Isolated mitochondria were kept in activity-preserving buffer (0.6 M sorbitol, 90 mM KCl, 15 mM KH_2PO_4, 20 mM Tris/HCl, 13 mM $MgSO_4$, 5 mM α-ketoglutarate, 1 mg/mL BSA, 4 mM ATP, 10 μg/mL pyruvate kinase, 5 mM phosphoenolpyruvate, 0.5 mM GTP) at 30 °C for 1 h and pelleted by

centrifugation at 4 °C, followed by scintillation counting. Because large amounts of mitochondria are required for export studies, the baseline export activity was measured independently and shown to be minimal.

1. Ardehali H, O'Rourke B, Marbán E (2005) Cardioprotective role of the mitochondrial ATP-binding cassette protein 1. *Circ Res* 97:740–742.
2. Warming S, Costantino N, Court DL, Jenkins NA, Copeland NG (2005) Simple and highly efficient BAC recombineering using galK selection. *Nucleic Acids Res* 33:e36.
3. Sohal DS, et al. (2001) Temporally regulated and tissue-specific gene manipulations in the adult and embryonic heart using a tamoxifen-inducible Cre protein. *Circ Res* 89:20–25.
4. Ardehali H, Chen Z, Ko Y, Mejía-Alvarez R, Marbán E (2004) Multiprotein complex containing succinate dehydrogenase confers mitochondrial ATP-sensitive K+ channel activity. *Proc Natl Acad Sci USA* 101:11880–11885.
5. Tangerås A, Flatmark T, Bäckström D, Ehrenberg A (1980) Mitochondrial iron not bound in heme and iron-sulfur centers. Estimation, compartmentation and redox state. *Biochim Biophys Acta* 589:162–175.
6. Ward JH, Jordan I, Kushner JP, Kaplan J (1984) Heme regulation of HeLa cell transferrin receptor number. *J Biol Chem* 259:13235–13240.
7. Gordon LI, et al. (2009) Blockade of the erbB2 receptor induces cardiomyocyte death through mitochondrial and reactive oxygen species-dependent pathways. *J Biol Chem* 284:2080–2087.

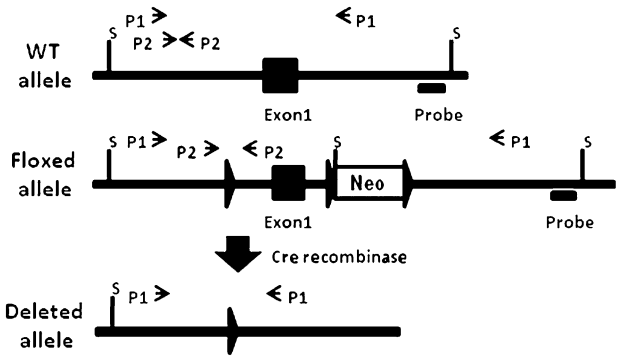

Fig. S1. Strategy for targeted disruption of ABCB8 gene. *Top*: WT allele with primers and a Southern blot probe-detection sites for the screening process. *Middle*: Structure of the targeted ABCB8 allele with insertion of a loxP sequence at 5′ end and loxP-Neo-loxP sequence at 3′ end of exon 1. LoxP sites are represented by triangles. *Bottom*: Deleted allele and removal of exon 1 after Cre-mediated recombination of loxP sequences. S, Sca I restriction endonuclease sites; Neo, neomycin selection cassette.

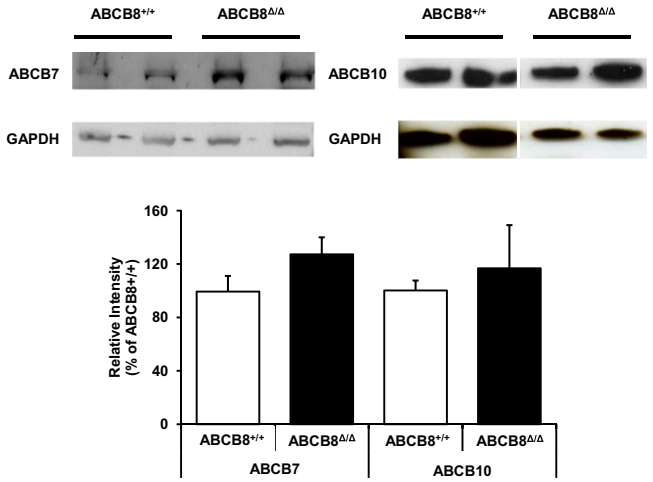

Fig. S2. Genetic ablation of ABCB8 does not result in a significant change in the levels of other mitochondrial ABC proteins. Representative Western blot images of ABCB7 and ABCB10 are shown (*Upper*) along with a summary of the densitometry analysis (*Lower*). Data are presented as mean ± SEM **P* < 0.05.

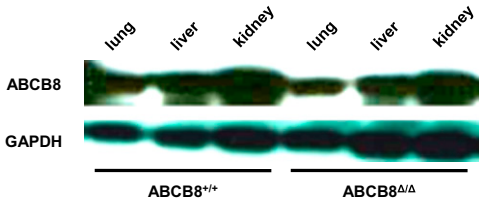

Fig. S3. Cardiac-specific KO of ABCB8 does not alter the levels of the protein in other tissues. Levels of ABCB8 in the lung, liver, and kidney tissues of ABCB8$^{\Delta/\Delta}$ mice are not different from those of WT animals.

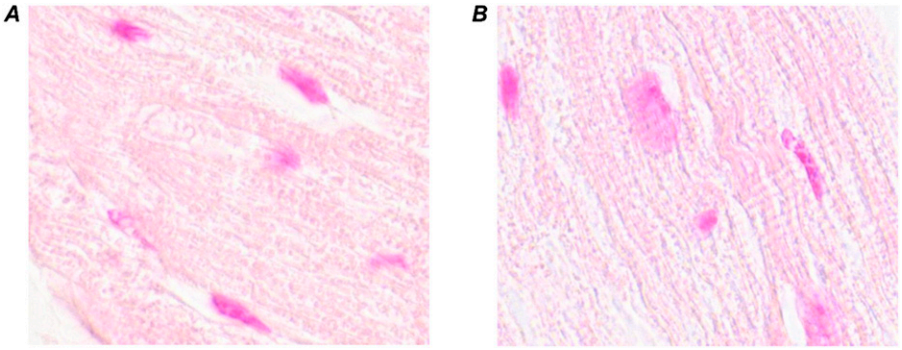

Fig. S4. Prussian blue staining of heart samples from WT (*A*) and ABCB8 KO (*B*) mice. ABCB8 KO hearts displayed enhancement of punctate purple staining, indicative of iron accumulation in the heart. Fuchsia pink is used as a counterstain.

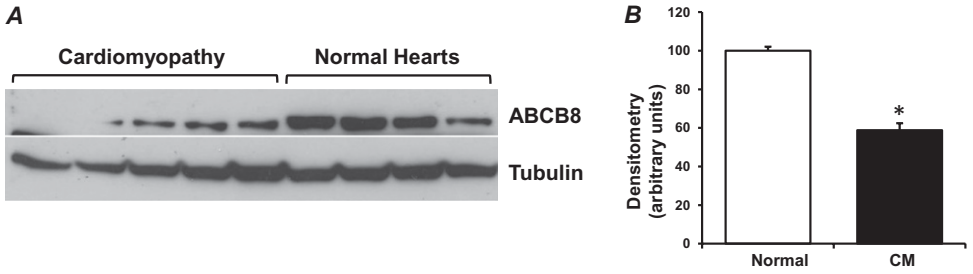

Fig. S5. ABCB8 levels are altered in cardiomyopathy. (*A*) Western blot showing ABCB8 expression in normal human hearts and explanted hearts from patients with end-stage cardiomyopathy. (*B*) Quantification of the Western blot (n = 4–5). Data are presented as mean ± SEM (*$P < 0.05$).

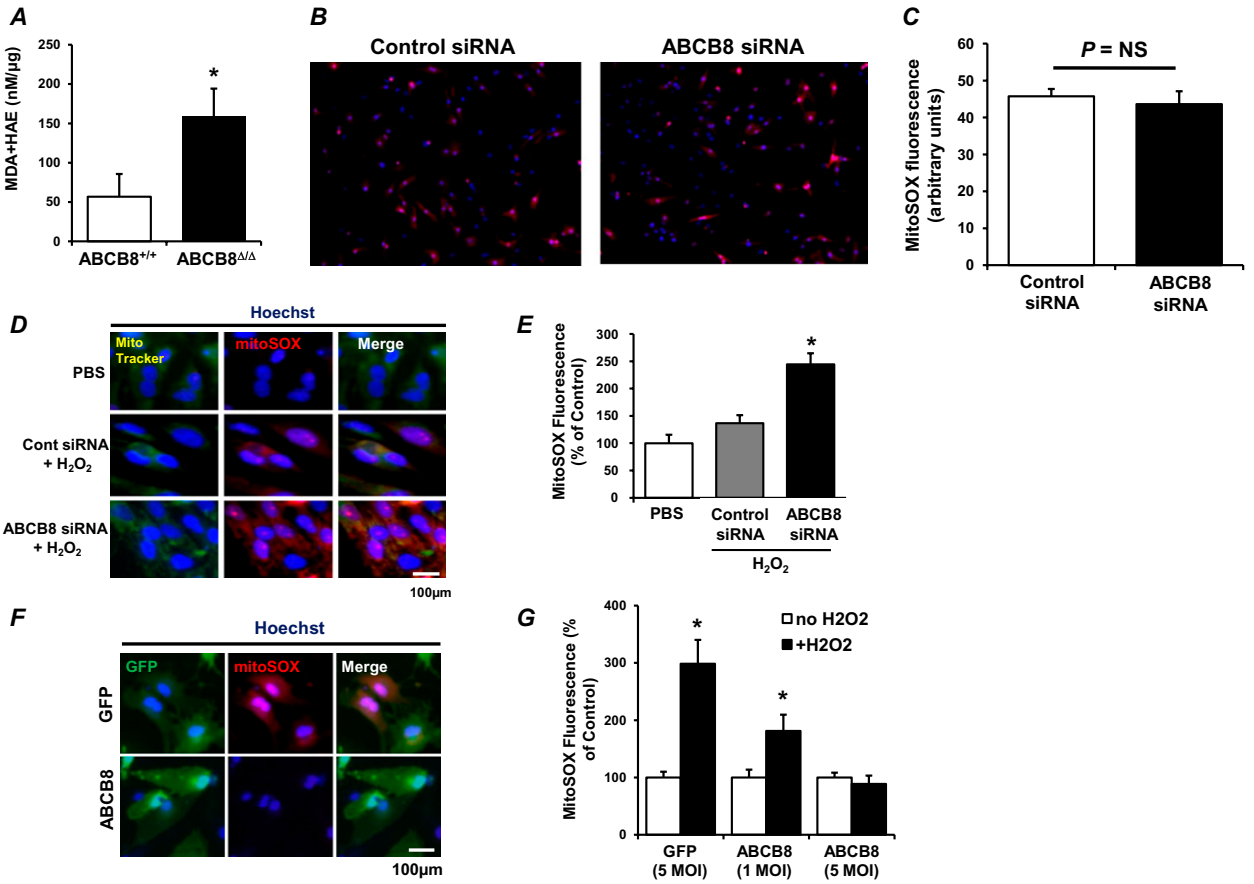

Fig. S6. Modulation of ABCB8 results in changes in the levels of ROS. (*A*) Levels of lipid peroxidation products (malondialdehyde; MDA and 4-hydroxyalkenals; HAE) in WT and ABCB8 knockout hearts ($n = 3$). (*B*) Representative confocal microscopy images showing fluorescence of MitoSOX in NRCM transfected with control and ABCB8 siRNA in the absence of H_2O_2. (*C*) ImageJ analysis of MitoSox fluorescence intensity. (*D*) Representative confocal microscopy images of MitoSOX red and MitoTracker green in NRCM transfected with control and ABCB8 siRNA in the presence of H_2O_2. In the laser scanning images, nuclei (blue) were counterstained with Hoechst 33342; 20× magnification. (*E*) FACS quantification of the intensity of MitoSOX fluorescence shows higher ROS in cells treated with ABCB8 siRNA after treatment with H_2O_2. (*F*) Representative confocal microscopy images showing MitoSOX Red fluorescence in NRCM transduced with GFP or ABCB8 adenovirus. (*G*) FACS quantification of the intensity of MitoSOX fluorescence ($n = 6$). Data are presented as mean ± SEM. *$P < 0.05$.

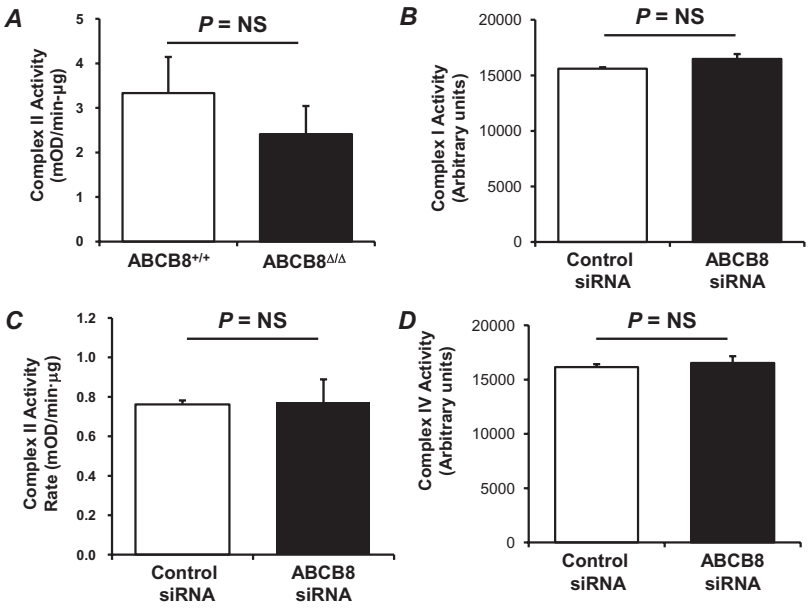

Fig. S7. A reduction in ABCB8 levels does not alter the activity of mitochondrial respiratory complexes. (*A*) Mitochondrial complex II activity ($n = 6$) in WT and ABCB8$^{D/D}$ hearts. Mitochondrial complex I ($n = 3$; *B*), II ($n = 6$; *C*), and IV ($n = 3$; *D*) activity in NRCMs treated with ABCB8 siRNA. The method used to measure complex I and IV activity was based on Sandwich ELISA Kit–Dipsticks assay (MitoSciences); thus, the *y* axis is reported as arbitrary units. Complex II assay was based on a microplate assay (MitoSciences). Data are presented as mean ± SEM.

Table S1. Primers used for quantitative RT-PCR analyses

Gene/primer	Sequence
18S	
Forward	5′-CGGGTCGGGAGTGGGT-3′
Reverse	5′-GAAACGGCTACCACATCCAAG-3′
mABC1 (rat)	
Forward	5′-GCTGGACAGCAGCTGAAAGG-3′
Reverse	5′-CTGGCCATAGACCTCTGTACTGTCT-3′
mABC1 (mouse)	
Forward	5′-GGGCAACAGGTGTAGCAGAT-3′
Reverse	5′-TGCTTGATAGCGTTCCTCCT-3′
ABCB7 (rat)	
Forward	5′-GGAGGAGGACTCCACACAGA-3′
Reverse	5′-ATGGCAACTCTGGCTCGCAG-3′
ABCB7 (mouse)	
Forward	5′-GGAGGAGGACTCCACACAGA-3′
Reverse	5′-ATGGCAACTCTGGCTCGCAG-3′
ABCB10 (rat and mouse)	
Forward	5′-CTGCTGAAGAACCCCAAAATTG-3′
Reverse	5′-GCTCGTTTTCGGCATCCA-3′